4th International Conference on Multiphase Flow, ICMF-2001
New Orleans, U.S.A., May 27-June 1, (2001), Paper No. 838

Discrete particle analysis of 2D pulsating fluidized bed

T. Kawaguchi, A. Miyoshi, T. Tanaka, Y. Tsuji

Department of Mechanical Engineering, Osaka University,
Yamada-Oka 2-1, Suita, Osaka, 565-0871, Japan

Abstract

The present paper describes a discrete particle simulation of pulsating fluidized beds. The effect of the gas pulsation on the flow pattern was studied numerically. Two cases of the bed were considered: one is of Group B particles in Geldart's classification and the other is of Group D particles. We also proposed a relaxation time of fluidized beds from the viewpoint of the bed response to the gas pulsation. The proposed relaxation time provided a good estimation to the present calculation results.

Keywords: Fluidized Bed; Pulsation; DEM; Numerical Simulation; Geldart's Classification

1. Introduction

It is known that when a particle bed are vibrated vertically, convective motion (e.g. Aoki et al., 1996) or bubble formation (Pak and Behringer, 1994) may be observed. A thin layer of particles vibrated vertically shows a variety of convective patterns depending on the frequency, the amplitude and the bed depth (Bizon et al., 1998). The pulsating fluidized bed, in which the gas velocity is oscillated temporally, is an equipment analogous to the vibrated bed. The pulsating fluidized bed is originally developed to fluidize cohesive particles (Moritomi et al., 1980). Köksal and Vural (1998) recently applied it to fluidized beds of coarse particles, and suggested that the size of bubbles in the fluidized bed can be controlled by the gas pulsation. The past studies on pulsating fluidized beds have focused on only the macroscopic fluidization state, such as avoiding channeling or the change of the bubble size. Then, there are very few studies which make more detailed mechanical discussions on the motion of particles and gas flow.

In the present work, a discrete particle analysis was performed on two-dimensional pulsating fluidized beds. The motion of all particles were traced by using DEM (Cundall and Strack, 1979). We performed calculations for two types of particles: Group B and Group D particles in Geldart's classification (Geldart, 1973). The effect of the gas pulsation on the particle motion was studied for each group of particles. The gas velocity was oscillated around the mean gas velocity at which the bubbling fluidization state was achieved. We analyzed the power spectrum of the horizontal distribution of the void fraction. It could characterize the spatial pattern in the horizontal direction. Furthermore, we tried to estimate the response of the bed from the relaxation time scale on the basis of the Ergun equation (Ergun, 1952).

2. Calculation

2.1 Fluid motion

Anderson and Jackson (1967) derived locally phase-averaged equations in which both the fluid and the solid phases are treated as continua. This set of equations provides basic equations for two-fluid models, and has been widely used in the numerical simulation of fluidized beds. We assumed fluid as inviscid following Gidaspow (1986). The basic equations for the fluid flow are as follows.

$$\frac{\partial}{\partial t}\varepsilon + \frac{\partial}{\partial x_j}(\varepsilon u_j) = 0 \tag{1}$$

$$\frac{\partial}{\partial t}(\varepsilon u_i) + \frac{\partial}{\partial x_j}(\varepsilon u_i u_j) = -\frac{\varepsilon}{\rho_g}\frac{\partial p}{\partial x_i} + \frac{\beta}{\rho_g}\left(\overline{v_{pi}} - u_i\right) \tag{2}$$

where ε is the void fraction, u_i is the fluid velocity, ρ_g is the fluid density, p is the pressure, and $\overline{v_{pi}}$ is the mean particle velocity in the control volume. The second term in the right hand side of Eq.(2) represents the interphase friction. The coefficient β was given by empirical correlations (see Gidaspow, 1986).

2.2 Particle motion

Newton's equation of motion was solved for each particles to obtain trajectories of particles. The gravity force $\boldsymbol{f}_G$, the interphase force (drag force) $\boldsymbol{f}_D$, and the interparticle force (contact force) $\boldsymbol{f}_C$ were taken into account. $\boldsymbol{f}_D$ was given by the following equation.

$$\boldsymbol{f}_D = \left\{ \frac{\beta}{1-\varepsilon}(\boldsymbol{u}-\boldsymbol{v}_p) - \frac{\partial p}{\partial \boldsymbol{x}} \right\} V_p \tag{3}$$

where V_p is the volume of a particle. The first term in Eq.(3) is the reaction force of the inter-phase friction in Eq.(2). The second term is a force caused by the pressure gradient. The contact force $\boldsymbol{f}_C$ was given by our previous model (Tsuji et al., 1993), in which linear elastic repulsion and constant restitution coefficient are assumed.

2.3 Calculation conditions

The parameters used in the present calculation are summarized in Table 1. The boundary conditions employed in the calculation are shown in Fig. 1. The gas is uniformly injected from the bottom of the bed. The magnitude of the gas velocity is oscillated sinusoidally around the mean velocity u_c with the frequency f_p and the amplitude A as follows.

$$u_0 = u_c + A\sin 2\pi f_p t \tag{4}$$

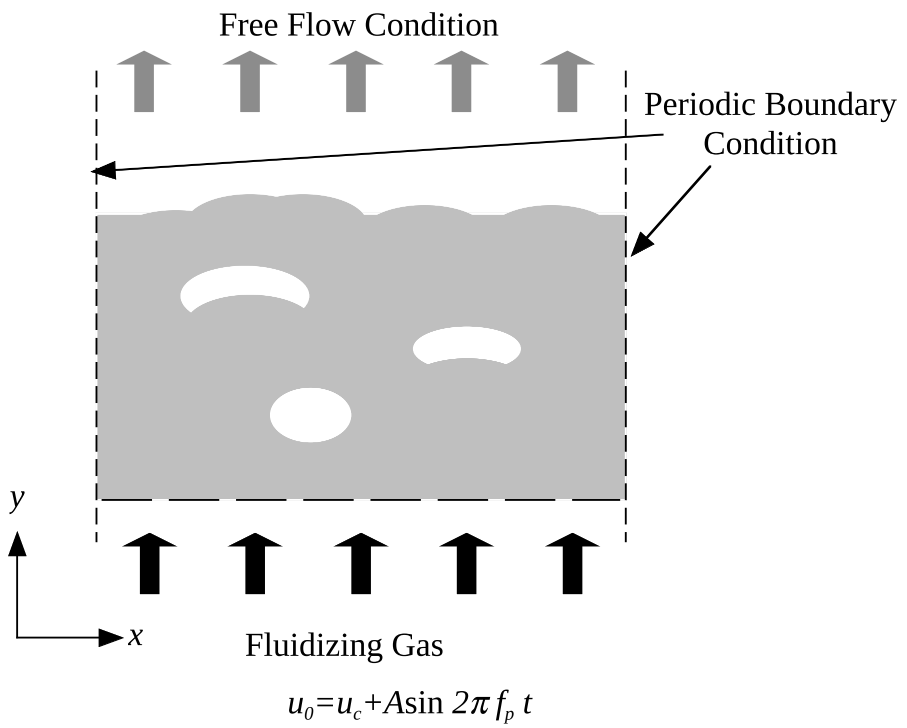

Fig. 1. Boundary condition

Table 1
Calculation conditions

classification		Group B	Group D
length between periodic boundaries (m)	L	0.2	1.35
initial height of gravity center (m)	H_{GI}	0.05	0.2
particle diameter (mm)	d_p	1.0	4.0
particle density (kg/m^3)	ρ_p	500	1000
number of particles	N_p	19800	40200
normal spring constant (N/m)	k_n	1000	
coefficient of friction (-)	μ_F	0.3	
coefficient of restitution (-)	e_p	0.9	
fluid density (kg/m^3)	ρ_g	1.205	
fluid viscosity (Pa s)	μ	1.81×10^{-5}	
mean gas velocity (m/s)	u_c	0.3	1.5
amplitude of pulsation (m/s)	A	0.15	0.5
frequency of pulsation (Hz)	f_p	0 - 30	0 - 15
size of control volume (mm)	$\Delta x \times \Delta y$	2.5 X 5.0	10 X 20
time step (msec)	Δt	0.01	0.1
minimum fluidization velocity (m/s)	u_{mf}	0.14	1.03
mean void fraction without pulsation (-)	ε_b	0.50	0.52

The periodic boundary condition was employed in the horizontal direction to eliminate the effect of side walls on the particle motion.

2.4 Power spectrum of voidage distribution

Taguchi (1995) analyzed a power spectrum of the particle velocity field in a vibrated bed, and showed that the power spectrum depends upon the wavenumber k as $k^{-5/3}$. In order to characterize the flow pattern in the fluidized bed, we analyzed a power spectrum of the horizontal distribution of the void fraction in the present work.

The calculation region was divided into 64 X 64 rectangular cells, and the void fraction was evaluated in each cell. The power spectrum of the horizontal distribution of the void fraction was given by the following equation.

$$E(\varepsilon,k)=\left\langle\left|\sum_{p}\varepsilon(p,q,t)\ \exp(-j2\pi k/l)\right|^{2}\right\rangle \quad (5)$$

where $\varepsilon(p,q,t)$ is the void fraction of the cell (p,q), k is the wavenumber, and l is the number of grids in the horizontal direction. The notation <...> represents time-averaging. Time-averaging over 2.0 s was applied. Spectra at four different vertical positions were calculated in the present work.

3. Results and discussion

3.1 Flow pattern for Group B particles

Fig. 2 shows snapshots of the particle motion for Group B particles. The deformation of

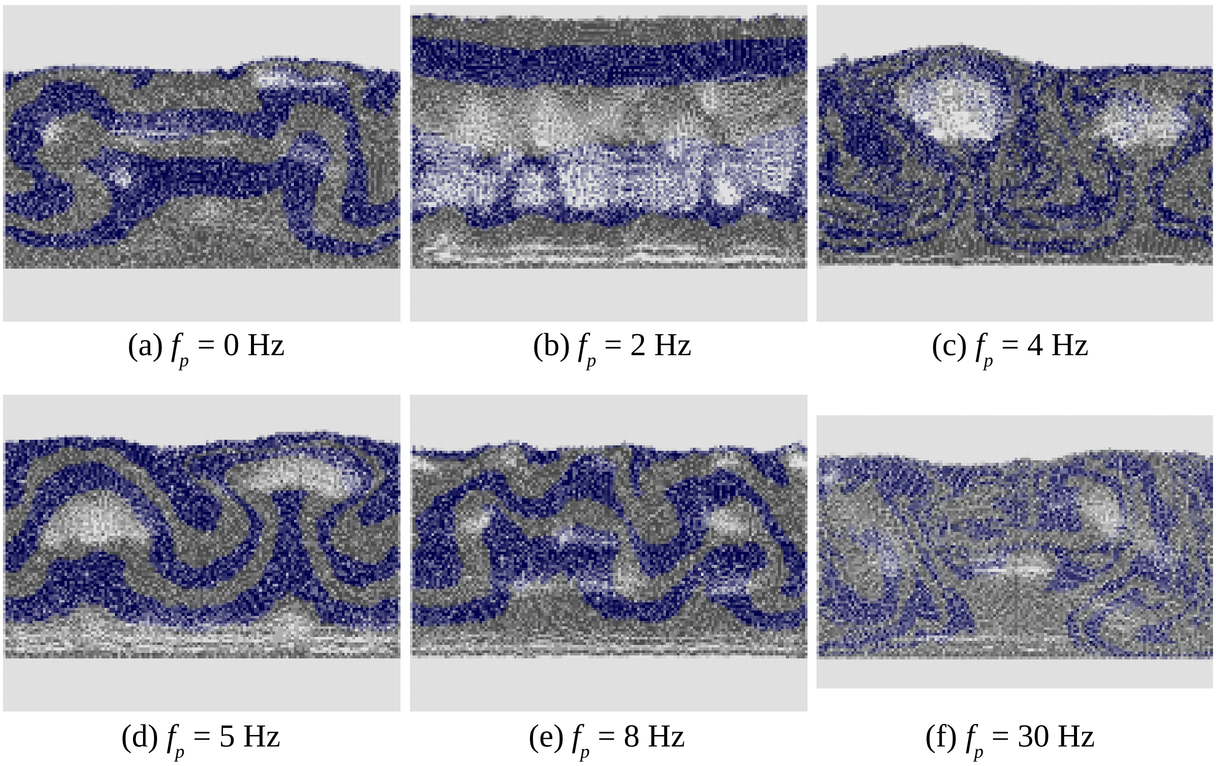

Fig. 2. Snapshot of particle motion : Group B particles.

the bed is visualized by colored layers. In Fig. 2 (a) f_p = 0 Hz, typical bubbling fluidization state, in which multiple bubbles exist in the bed, was obtained. In Fig. 2 (b) f_p = 2 Hz, the bed simply oscillated vertically with large amplitude synchronizing the frequency of the gas pulsation. In Fig. 2 (c) f_p = 4 Hz and (d) f_p = 5 Hz, two large bubbles can be found at two different horizontal positions in the bed. We found that this flow pattern was stably repeated in the calculation. In Fig. 2 (e) f_p = 8 Hz and (f) f_p = 30 Hz, the size of bubbles becomes small again, and the flow pattern for these frequencies are similar to that for f_p = 0 Hz.

The power spectra of the horizontal distribution of the void fraction, $E(\varepsilon,k)$, at four different vertical positions, H, are shown in Fig. 3. The spectrum for f_p = 2 Hz is relatively flat compared to those for the other frequencies. This means that no characteristic structures exist in the horizontal direction at f_p = 2 Hz. It corresponds to the particle motion in Fig. 2. In Fig. 3 (c) f_p = 4 Hz and (d) f_p = 5 Hz, the spectra have a remarkable peak at k = 2. It corresponds to the flow pattern for these frequencies; i.e. two large bubbles are generated at two different horizontal

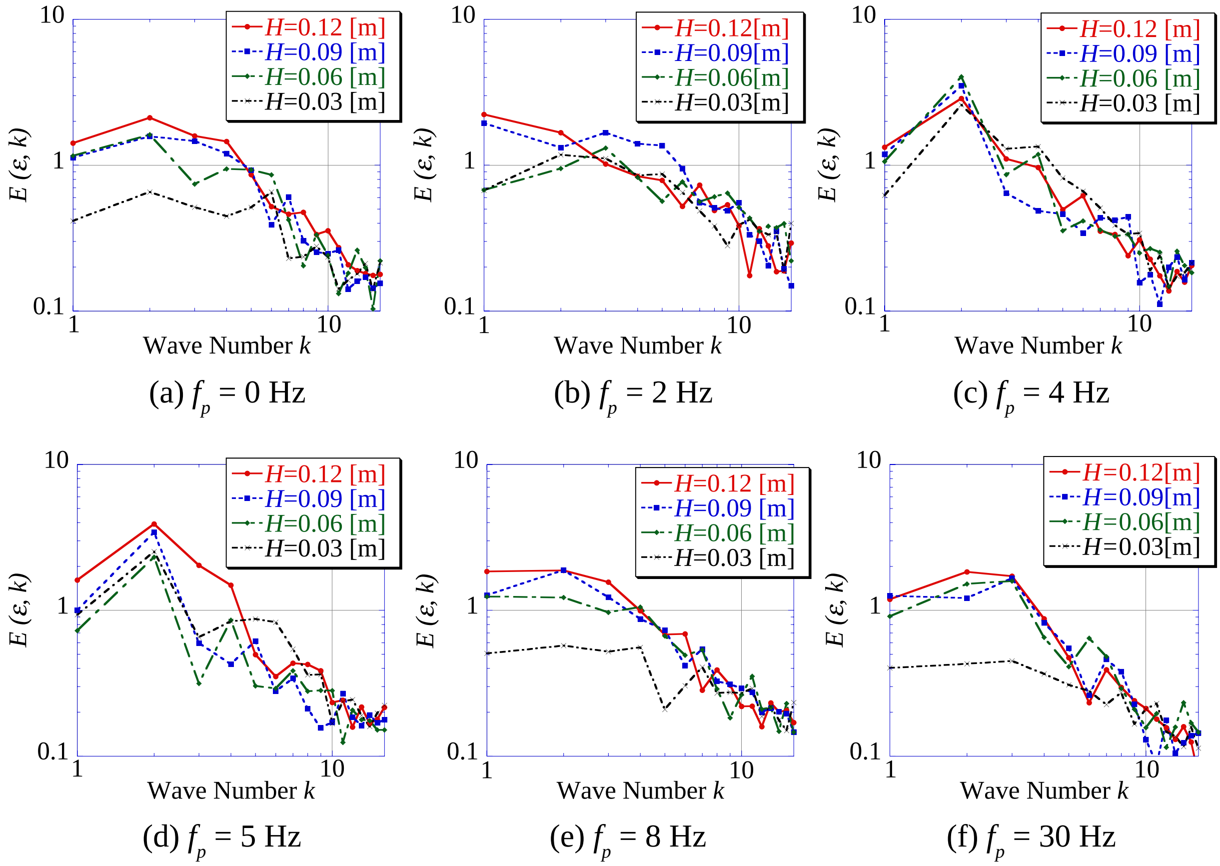

Fig. 3. Power spectrum of voidage distribution : Group B particles.

positions. The spectra for f_p = 0 Hz, f_p = 8 Hz and f_p = 30 Hz are similar to one another. That is, the power is strong in the low-wavenumber region ($k \leq 4$), while the spectra have no clear peaks. Furthermore the higher the vertical position is, the stronger the power becomes. It means that bubbles grow with the height and become clear at higher positions.

We can summarize the effect of the gas pulsation on the flow pattern for Group B particles as follows. The effect of the gas pulsation on the flow pattern is outstanding at f_p = 4 - 5 Hz. The gas pulsation can stabilize the bubble formation.

3.2 Flow pattern for Group D particles

Fig. 4 shows snapshots of particle motion for Group D particles. In Fig. 4 (a) f_p = 0 Hz, typical bubbling fluidization was obtained also for Group D particles. In Fig. 4 (b) f_p = 1 Hz and (c) f_p = 2 Hz, the size of bubbles is much larger than that for f_p = 0 Hz. For f_p > 4 Hz, the size of bubbles become small again, and the flow pattern is similar to that for f_p = 0 Hz.

The power spectra of the horizontal distribution of the void fraction, $E(\varepsilon,k)$, at four different vertical positions are shown in Fig. 5. In Fig. 5 (b) f_p = 1 Hz and (c) f_p = 2 Hz, the spectra have the maximum value at k = 1, and decrease with k. This corresponds to the flow pattern in Fig. 4

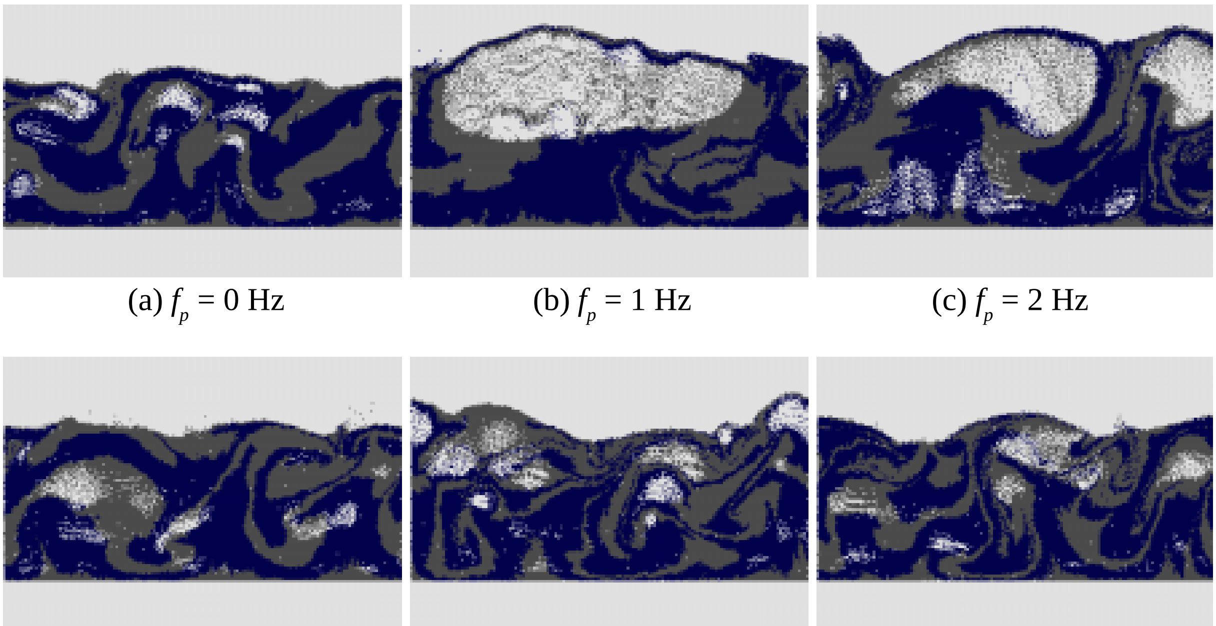

(a) f_p = 0 Hz (b) f_p = 1 Hz (c) f_p = 2 Hz

(d) f_p = 4 Hz (e) f_p = 8 Hz (f) f_p = 15 Hz

Fig. 4. Snapshot of particle motion : Group D particles.

(b) and (c). That is, only one or two large bubble(s) is (are) generated in the bed for these frequencies. For f_p = 0 Hz and $f_p \geq 4$ Hz, the spectra do not have any clear peaks. The power is strong for k = 1 - 4 and decrease with k for $k > 5$. It means that the number of bubbles in the bed varies from 1 to 4 temporally.

3.3 Relaxation time scale of the bed

Comparing the results in the sections *3.1* and *3.2*, the response of the particle bed to the gas pulsation might depend on the particle properties. We propose a relaxation time of the be to estimate the response of the bed to the gas pulsation.

It is known that the Ergun equation can provide the pressure drop across the particle bed for the wide range of packing state. By linearizing the fluid drag force per unit volume of a bed, $F(u)$, around $u = u_{mf}$, we define the relaxation time of the bed. Applying the Taylor expansion to

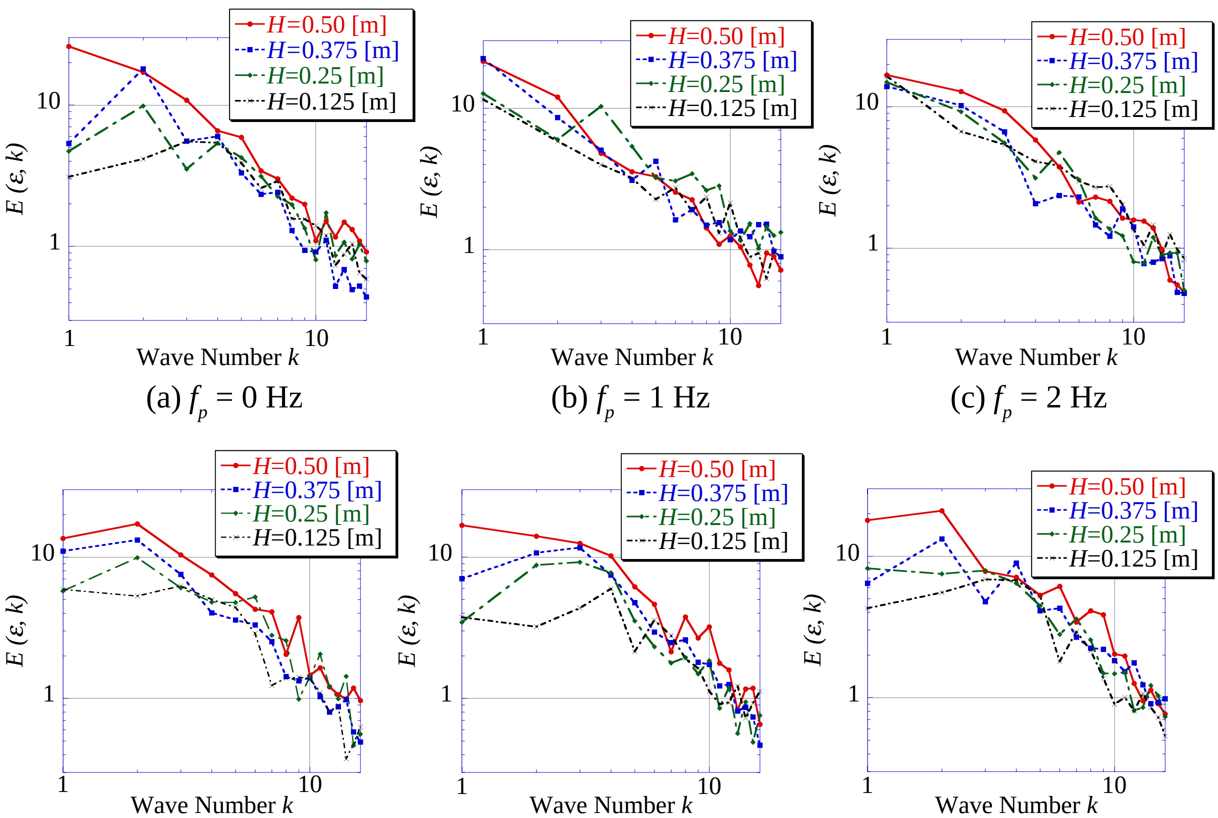

(a) f_p = 0 Hz (b) f_p = 1 Hz (c) f_p = 2 Hz

(d) f_p = 4 Hz (e) f_p = 8 Hz (f) f_p = 15 Hz

Fig. 5. Power spectrum of voidage distribution : Group D particles.

$F(u)$ at $u = u_{mf}$, and neglecting $O(\Delta u^2)$ or higher order terms, we obtained the following linearized equation.

$$F(u_{mf} + \Delta u) = F(u_{mf}) + \left.\frac{dF}{du}\right|_{u_{mf}} \Delta u \tag{6}$$

The first term on the right hand side is the fluid drag force at $u = u_{mf}$, which is balanced with the gravity force per unit volume. Thus, we have $F(u_{mf}) = Mg$, where $M = (1-\varepsilon_b)\rho_p$, the mass of the bed per unit volume. By substituting this equation and the Ergun equation into Eq. (6), we get,

$$F(u_{mf} + \Delta u) - Mg = A(B + 2Cu_{mf})\Delta u \tag{7}$$

where $A = \dfrac{1-\varepsilon_b}{d_p \varepsilon_b{}^3}$, $B = \dfrac{150(1-\varepsilon_b)\mu}{d_p}$, $C = 1.75\rho_g$. ε_b is the void fraction at the fluidizing state with $f_p = 0$ Hz, and is calculated as follows.

$$\varepsilon_b = 1 - \frac{N_p V_p}{2\overline{H_G} d_p L} \tag{8}$$

where N_p is the number of particles, and L is the length between periodic boundaries. Then, the equation of motion of a bed for a small variation in gas velocity Δu from u_{mf} is obtained by the following equation.

$$M\frac{d^2 y}{dt^2} = \alpha \cdot \Delta u \tag{9}$$

where $\alpha = A(B+2C\,u_{mf})$. Here, the bed is assumed as a rigid body. Then, the excess fluid drag force exerted by Δu is as follows.

$$\left.\frac{d^2 y}{dt^2}\right|_{t=0} = \Delta u \times \frac{\alpha}{M} \tag{10}$$

Thus the relaxation time τ_b is given by

$$\tau_b = \frac{M}{\alpha} \tag{11}$$

By substituting $\varepsilon_b = 0.50$ and $u_{mf} = 0.14$ m/s for Group B particles into Eq.(11), we obtain $\tau_b =$ 0.032 s. Analogously, by substituting $\varepsilon_b = 0.52$ and $u_{mf} = 1.03$ m/s for Group D particles into Eq.(11), we obtain $\tau_b = 0.120$ s. These relaxation times correspond to about four times of frequency at which the pulsation effect on the flow pattern saturate for each cases. This relaxation time of the bed could provide an estimation of dynamic response of the bed to the gas pulsation.

4. Conclusions

(1) For Group B particles, the effect of the gas pulsation on the flow pattern is outstanding at f_p = 4 - 5 Hz. Two large bubbles are stably generated in the bed at f_p = 4 - 5 Hz. The effect of the gas pulsation on the particle motion saturates at f_p > 8 Hz.

(2) For Group D particles, the size of bubbles becomes large at f_p = 1 - 2 Hz. The effect of the gas pulsation on the particle motion saturates at f_p > 4 Hz.

(3) We propose a relaxation time of the bed on the basis of the Ergun equation. As far as the present calculated results are concerned, our relaxation time could provide a good estimation of dynamic response of the bed to the gas pulsation.

Acknowledgments

This work is partially founded by the Japanese Ministry of Education, Science, Sports and Culture, Grant-in-Aid for Encouragement of Young Scientists (A) (12750140).

References

Aoki,K.M., Akiyama,T., Maki,Y., Watanabe,T., 1996. Convective roll patterns in vertically vibrated beds of granules. Phys.Rev.E. 54-1, 874-883.

Anderson,T.B., Jackson,R., 1967. A fluid mechanical description of fluidized bed. I&EC Fundamentals, 6-4, 527-539.

Bizon,C., Shattuck,M.D., Swift,J.B., McCormick,W.D., Swinney,H.L., 1998. Patterns in 3D vertically oscillated granular layers: simulation and experiment. Phys.Rev.Lett. 80-1. 57-60.

Cundall,P.A., Strack,O.D.L., 1979. Discrete numerical model for granular assemblies. Géotechnique. 29-1. 47-65.

Ergun,S., 1952. Fluid flow through packed columns. Chem.Engng.Prog. 48-2. 89-94.

Geldart,D., 1973. Types of gas fluidization. Powder Technology. 7. 285-292.

Gidaspow,D., 1986. Hydodynamics of fluidization and heat transfer: supercomputer modeling. Appl.Mech.Rev. 39-1. 1-23.

Köksal,M., Vural,H., 1998. Bubble size control in a two-dimensional fluidized bed using a moving double plate distributor. Powder Technology. 95. 205-213.

Moritomi,H., Mori,S., Araki,K., Moriyama,A., 1980. Periodic pressure fluctuation in a gaseous fluidized bed. Kagaku Kogaku Ronbunshu. 6-4. 392-396. (in Japanese)

Pak,H.K., Behringer,P.R., 1994. Bubbling in vertically vibrated granular materials. Nature. 371. 231-233.

Taguchi,Y-h., 1995. Numerical study of granular turbulence and the appearance of the $k^{-5/3}$ energy spectrum without flow. Physica D. 80. 61-71.

Tsuji,Y., Kawaguchi,T., Tanaka,T., 1993. Discrete particle simulation of two-dimensional fluidized bed. Powder Technology. 77. 79-87.